



Since January 2020 Elsevier has created a COVID-19 resource centre with free information in English and Mandarin on the novel coronavirus COVID-19. The COVID-19 resource centre is hosted on Elsevier Connect, the company's public news and information website.

Elsevier hereby grants permission to make all its COVID-19-related research that is available on the COVID-19 resource centre - including this research content - immediately available in PubMed Central and other publicly funded repositories, such as the WHO COVID database with rights for unrestricted research re-use and analyses in any form or by any means with acknowledgement of the original source. These permissions are granted for free by Elsevier for as long as the COVID-19 resource centre remains active.



## Role of the viral hemagglutinin in the anti-influenza virus activity of newly synthesized polycyclic amine compounds



Eva Torres<sup>a</sup>, María D. Duque<sup>a</sup>, Evelien Vanderlinden<sup>b</sup>, Chunlong Ma<sup>c,d</sup>, Lawrence H. Pinto<sup>c</sup>, Pelayo Camps<sup>a</sup>, Mathy Froeyen<sup>b</sup>, Santiago Vázquez<sup>a,\*</sup>, Lieve Naesens<sup>b,\*</sup>

<sup>a</sup> Laboratori de Química Farmacèutica (Unitat Associada al CSIC), Facultat de Farmàcia, and Institute of Biomedicine (IBUB), Universitat de Barcelona, Av. Diagonal 643, Barcelona E-08028, Spain

<sup>b</sup> Rega Institute for Medical Research, KU Leuven, 3000 Leuven, Belgium

<sup>c</sup> Department of Neurobiology and Physiology, Northwestern University, Evanston, IL 60208-3500, United States

<sup>d</sup> Department of Molecular Biosciences, Northwestern University, Evanston, IL 60208-3500, United States

### ARTICLE INFO

#### Article history:

Received 29 January 2013

Revised 13 May 2013

Accepted 12 June 2013

Available online 22 June 2013

#### Keywords:

Amantadine  
Hemagglutinin  
Influenza A virus  
M2 protein  
Polycyclic amines

### ABSTRACT

We here report on the synthesis of new series of polycyclic amines initially designed as ring-rearranged analogs of amantadine and featuring pentacyclo-, hexacyclo-, and octacyclo rings. A secondary amine, 3-azaheptacyclo[7.6.0.0<sup>1,5</sup>.0<sup>5,12</sup>.0<sup>6,10</sup>.0<sup>11,15</sup>]pentadeca-7,13-diene, **3**, effectively inhibited A/M2 proton channel function, and, moreover, possessed dual activity against an A/H3N2 virus carrying a wild-type A/M2 proton channel, as well as an amantadine-resistant A/H1N1 virus. Among the polycyclic amines that did not inhibit influenza A/M2 proton channel function, several showed low-micromolar activity against tested A/H1N1 strains (in particular, the A/PR/8/34 strain), but not A/H3N2 influenza viruses. A/PR/8/34 mutants selected for resistance to these compounds possessed mutations in the viral hemagglutinin that markedly increased the hemolysis pH. Our data suggest that A/H1N1 viruses such as the A/PR/8/34 strain are particularly sensitive to a subtle increase in the endosomal pH, as caused by the polycyclic amine compounds.

© 2013 Elsevier B.V. All rights reserved.

## 1. Introduction

Adamantane derivatives are of significant interest in medicinal chemistry (Lamoureux and Artavia, 2010; Liu et al., 2011). For example, amantadine (Amt) and rimantadine have been used for many years as anti-influenza A virus agents (Jefferson et al., 2006; Alves Galvão et al., 2012); adapalene is a topical retinoid used to treat skin diseases such as acne (Piérard et al., 2009); and vildagliptin and saxagliptin were recently approved for type 2 diabetes (Vilhauer et al., 2003; Augeri et al., 2005). Moreover, Amt and its dimethyl derivative memantine are NMDA receptor antagonists approved for the treatment of Parkinson's and Alzheimer's disease, respectively (Lipton, 2006; Hubsher et al., 2012) (Fig. 1).

*Abbreviations:* Amt, amantadine; CPE, cytopathic effect; HRMS, high resolution mass spectra; MDCK, Madin–Darby canine kidney; MTS, 3-(4,5-dimethylthiazol-2-yl)-5-(3-carboxymethoxyphenyl)-2-(4-sulfophenyl)-2H-tetrazolium; HA, hemagglutinin; NMDA, N-methyl-D-aspartate; TEV, two-electrode voltage clamps; TM, transmembrane; wt, wild-type.

\* Corresponding authors. Tel.: +34 934024533; fax: +34 934035941 (S. Vázquez), tel.: +32 16337345; fax: +32 16337340 (L. Naesens).

E-mail addresses: [svazquez@ub.edu](mailto:svazquez@ub.edu) (S. Vázquez), [lieve.naesens@rega.kuleuven.be](mailto:lieve.naesens@rega.kuleuven.be) (L. Naesens).

The anti-influenza A virus activity of Amt and rimantadine is based on inhibition of the proton channel function of the viral A/M2 protein (Hay et al., 1985). This homotetrameric type III integral membrane protein contains a small N-terminal ectodomain (23 residues), a helical transmembrane domain (20 residues), which forms the pore of the proton channel, and a long C-terminal cytoplasmic tail (53 residues) (Hong and DeGrado, 2012; Pinto and Lamb, 2006; Wang et al., 2011b). The A/M2 protein has different functions in the viral life cycle [including a role in virus assembly and budding (Rossman and Lamb, 2011)], but its critical role during virus entry is situated after the virions have entered the host cell by endocytosis. Namely, proton transport by A/M2 is required for acidification of the virion interior and uncoating of the viral genome (Cady et al., 2009; Hu et al., 2010; Pinto and Lamb, 2006; Sharma et al., 2010). The low pH inside the endosomes not only activates the A/M2 proton channel, but also induces an irreversible conformational change of the viral hemagglutinin (HA), leading to displacement of its hydrophobic fusion peptide in the direction of the target membrane, and fusion of the viral and endosomal membranes (Cross et al., 2001a). After the viral genome segments have been released through the fusion pore into the cytoplasm, they are transported to the nucleus to initiate RNA transcription and replication.

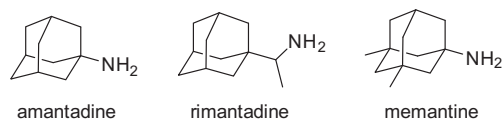


Fig. 1. Chemical structures of amantadine (Amt); rimantadine and memantine.

Recent studies (Cady et al., 2010, 2011; Rosenberg and Casarotto, 2010; Stouffer et al., 2008) have identified the binding sites for Amt and rimantadine within the A/M2 channel pore. These structural insights also provide an explanation for the intrinsic inactivity of these drugs against influenza B virus, as well as their viral resistance profile. Most currently circulating influenza A/H1N1 and A/H3N2 viruses are Amt-resistant mutants, carrying substitutions in the transmembrane region of A/M2 that reduce the binding of Amt, in particular: S31N, V27A and L26F (Bright et al., 2005, 2006; [www.cdc.gov/flu/](http://www.cdc.gov/flu/)). In the USA, Amt resistance increased from 1.9% in 2004 to 92.3% in December 2005 (Bright et al., 2006) and, in 2006, the Centers for Disease Control and Prevention recommended against use of Amt for treatment or prophylaxis of influenza (Smith et al., 2006; Fiore et al., 2011). For these reasons, there is an urgent need for new Amt analogs that are effective against most common Amt-resistant influenza virus mutants. Significant progress in this field was very recently made by the discovery of polycyclic amine derivatives which are active against M2 channels carrying a V27A, L26F or S31N mutation. Spiroadamantane analogues having a larger size than amantadine were found able to block the M2 channel, even when its space is increased by the V27A or L26F substitution (Wang et al., 2011a). Likewise, inhibition of an M2 channel carrying the S31N mutation, which increases the polarity of the cavity, was accomplished by designing amantadine–isoxazole conjugates (Wang et al., 2013). Whether a similar mode of action may apply to an imidazole-linked amantadine analogue reported to have equal activity against wild-type and S31N-mutant M2, remains to be investigated (Zhang et al., 2010a). During the past years, our group has synthesized several polycyclic Amt analogs containing different scaffolds, including ring-contracted (Camps et al., 2008), ring-rearranged (Duque et al., 2011) and 2,2-dialkyl (Torres et al., 2012) derivatives of Amt (Fig. 2). A first series of ring-rearranged analogs of Amt consisting of amines **1**–**5** and their derivatives **7** (a tertiary amine), **8** (an amidine) and **19** (a secondary amine), was evaluated for inhibition of A/M2 proton channel activity, by using the conductance assay in M2-expressing oocytes (Duque et al., 2011). The secondary amines **3** and **5** (Fig. 2) displayed similar IC<sub>50</sub> values for wt A/M2 as Amt, but, unfortunately, were inactive against the Amt-resistant S31N or V27A mutant forms of A/M2 (Duque et al., 2011). It was also found that the tertiary amine **7**, a diethyl derivative of **1**, had minimal, if any, activity against the wt A/M2 protein in the M2 conductance assay. Strikingly, we now found that **7** displays low micromolar activity against the influenza A/PR/8/34 (A/H1N1) strain in cell culture. Since this strain carries two Amt resistance mutations in its A/M2 protein, a mode of action unrelated to

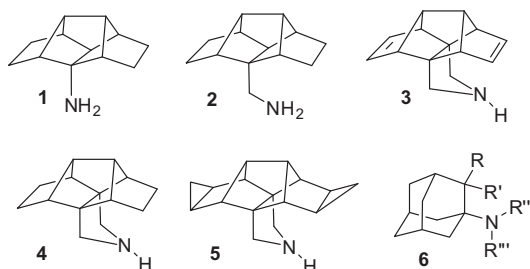


Fig. 2. Different polycyclic amine scaffolds previously synthesized by our group.

A/M2 inhibition should apply to compound **7**. This intriguing subtype-dependent activity against A/H1N1 viruses (in particular, strain A/PR/8/34) was also observed with a recent series of 2,2-dialkylamantadine derivatives of general structure **6** (Torres et al., 2012) (Fig. 2).

In the present report, we first describe the synthesis of a novel series of pentacyclic, hexacyclic and octacyclic alkylated amines, amidines and guanidines derived from amines **1**–**5**. Intrigued by the finding that, alike several other polycyclic amines, these compounds were again active against A/H1N1 but not A/H3N2 viruses, we performed broad anti-influenza virus testing, and selection and characterization of resistant viruses. Our results indicate that the polycyclic amines interfere with HA-mediated fusion by causing subtle increases in the endosomal pH, and that A/H1N1 viruses such as A/PR/8/34 are particularly sensitive to this pH effect.

## 2. Materials and methods

### 2.1. General methods for chemical synthesis

Melting points were determined in open capillary tubes with a MFB 595010M Gallenkamp melting point apparatus. 400 MHz <sup>1</sup>H NMR and 100.6 MHz <sup>13</sup>C NMR spectra were recorded on a Varian Mercury 400 spectrometer and 500 MHz <sup>1</sup>H NMR and 125.7 MHz <sup>13</sup>C NMR spectra were performed on a Varian Inova 500 equipment. Except where otherwise stated, <sup>1</sup>H NMR (500 MHz) and <sup>13</sup>C NMR (100.6 MHz) spectra were carried out in CD<sub>3</sub>OD solution. The chemical shifts are reported in ppm (δ scale) relative to internal tetramethylsilane, and coupling constants are reported in hertz (Hz). Assignments given for the NMR spectra of the new compounds are based on DEPT, COSY <sup>1</sup>H/<sup>1</sup>H (standard procedures), and COSY <sup>1</sup>H/<sup>13</sup>C (gHSQC and gHMBC sequences) experiments for selected compounds. IR spectra were run on a Perkin–Elmer Spectrum RX I spectrophotometer always in KBr. Absorption values are expressed as wavenumbers (cm<sup>-1</sup>); only significant absorption bands are given. For the MS and GC/MS analyses the sample was introduced directly or through a gas chromatograph, respectively using a Hewlett–Packard 5988A mass spectrometer. For GC/MS analyses a 30-meter column [5% diphenyl–95% dimethylpolysiloxane, conditions: 10 psi, initial temperature: 35 °C (2 min), then heating at a range of 8 °C/min till 300 °C, then isothermic at 300 °C] was used. The electron impact (70 eV) or chemical ionization (CH<sub>4</sub>) techniques were used. The high resolution mass spectra were carried out with a Micromass Autospec or a LC/MSD TOF Agilent Technologies spectrometers. Column chromatography was performed on silica gel 60 AC.C (35–70 mesh, SDS, ref 2000027). Thin-layer chromatography was performed with aluminum-backed sheets with silica gel 60 F254 (Merck, ref 1.05554), and spots were visualized with UV light and 1% aqueous solution of KMnO<sub>4</sub>. The analytical samples of all of the new compounds that were subjected to pharmacological evaluation possess a purity of >95%, as evidenced by results of their <sup>1</sup>H NMR spectra and elemental analyses.

### 2.2. Compound synthesis

Detailed compound synthesis and characterization can be found in the [Supplementary data](#).

### 2.3. Biological experiments

#### 2.3.1. Inhibition of A/M2 proton channel function by two-electrode voltage clamp analysis

The cDNA encoding the influenza A/M2 protein from the A/Udm/72 strain was inserted into a pGEM3 vector, for expression

on oocyte plasma membranes. The S31N and V27A mutant forms of A/M2 were generated by the QuikChange site-directed mutagenesis kit (Agilent Technologies). Synthesis of mRNA and microinjection of oocytes were carried out as described (Ma et al., 2008). At 48–72 h after mRNA injection, macroscopic recording of the membrane current was performed (Balannik et al., 2009). When the inward current reached maximum, various concentrations of the test compounds were added at pH 5.5. The compounds were applied for 2 min, and the residual membrane current was compared with the membrane current before compound application. Data were analyzed with pCLAMP 10.0 software (Axon Instruments, Sunnyvale, CA).

### 2.3.2. Cell culture assays for antiviral activity and cytotoxicity

The antiviral activity of the compounds was determined in established CPE reduction assays, using a diverse set of DNA and RNA viruses as indicated, and including three (sub)types of influenza virus: A/Puerto Rico/8/34 (A/H1N1); A/Hong Kong/7/87 (A/H3N2) and B/Hong Kong/5/72 (Naesens et al., 2009; Vanderlinden et al., 2010). Some compounds were additionally tested against the influenza virus strains: A/Ned/378/05 (A/H1N1); A/FM/1/47 (A/H1N1); A/Virginia/ATCC3/2009 (2009 pandemic A/H1N1); A/Ishikawa/7/82 (A/H3N2) and A/X-31 (A/H3N2). All details on the origin of these viruses and antiviral testing procedures can be found elsewhere (Vanderlinden et al., 2010, 2012). Briefly, Madin-Darby canine kidney cells seeded in 96-well plates were exposed to influenza virus [multiplicity of infection: 50 CCID<sub>50</sub> (50% cell culture infective dose) per well] together with the test compounds. After three days incubation at 35 °C, microscopy was performed to score the virus-induced cytopathic effect (CPE) as well as compound cytotoxicity. These data were confirmed by the colorimetric formazan-based MTS cell viability assay. Antiviral activity was expressed as the EC<sub>50</sub> value, or compound concentration producing 50% inhibition of the virus-induced CPE, as determined by microscopy or MTS assay. Compound cytotoxicity was expressed as the minimum inhibitory concentration (MCC), i.e. the concentration producing minimal changes in cell morphology, or the CC<sub>50</sub> value, i.e. the concentration causing 50% reduction in cell viability by MTS assay.

To determine the effect of the compounds on virus yield, MDCK cells were incubated with influenza virus (strain A/PR/8/34) and compounds as above, and the supernatants were collected at day 3 p.i. Serial (5-fold) dilutions of these samples were added to MDCK cells seeded in 96-well plates. After 3 days incubation, the viral CPE was scored by microscopy and the virus titer was calculated by the CCID<sub>50</sub> method of Reed and Muench (1938).

### 2.3.3. Selection and characterization of resistant mutants

The influenza virus strain A/PR/8/34 was passed on MDCK cells in the presence of **4** or **6c**, or in the absence of test compound. With each passage, the virus-containing supernatant was collected from wells showing clear CPE at day 3 post infection. This virus was applied to fresh MDCK cells with further addition of compound at gradually increasing concentrations (up to 150 μM). After seven passages, the harvested virus was plaque-purified in MDCK cells. From each condition (**4**, **6c** or no compound), three individual clones were collected and expanded in MDCK cells. The virus clones were subjected to full HA gene sequencing using UTR-directed outer primers (Hoffmann et al., 2001) as well as custom-synthesized inner primers. The antiviral sensitivity of the mutant viruses was determined with the CPE reduction assay described above.

### 2.3.4. Determination of virus hemolysis pH

A published procedure was used to determine the pH of erythrocyte hemolysis (Vanderlinden et al., 2010). Briefly, allantoic

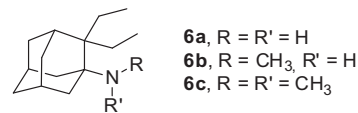


Fig. 3. 2,2-Diethylamantadine derivatives with activity against influenza A/H1N1 strains.

influenza virus stock and chicken red blood cells (RBC) were incubated at 37 °C for 10 min. After centrifugation, the RBC pellets were resuspended in PBS. The pH was lowered to 4.6–6.0 by addition of 1 N acetic acid, and the samples were incubated at 37 °C for 25 min. Then, the reaction was neutralized with NaOH, and intact RBC were removed by centrifugation. The supernatant was transferred to a 96-well plate and the optical density was measured at 540 nm. Background values were derived from mock-infected samples undergoing identical treatment. The pH of erythrocyte hemolysis was expressed as the pH at which 50% hemolysis occurs, relative to the value at pH 4.6.

## 3. Results

### 3.1. Chemical synthesis of ring-rearranged analogs of Amt 7–19, rimantadine analog 22 and pyrrolidine derivatives 23–31

Starting from primary amine **1**, we previously performed the synthesis of tertiary amine **7** and acetamidine **8** (Duque et al., 2011). To further explore the effect of alkylation on the biological activity, **1** was treated with formaldehyde and NaCNBH<sub>3</sub>, to obtain tertiary amine **9** in 78% yield, while treatment of **1** with thiophene-2-carboxaldehyde and NaCNBH<sub>3</sub> led to **10** in 75% yield (Fig. 4).

Similarly, from primary amine **2**, reductive alkylation with thiophene-2-carboxaldehyde, benzaldehyde, formaldehyde or acetaldehyde and NaCNBH<sub>3</sub> led to amines **11**, **12**, **13** and **14**, respectively, in high yield. Alkylation of **2** with 1,5-dibromopentane led to piperidine derivative **16** in 54% yield. Reductive methylation of secondary amine **12** with formaldehyde and NaCNBH<sub>3</sub> led, in 82% yield, to tertiary amine **15**, which on catalytic hydrogenation quantitatively furnished secondary amine **19**, that had been previously synthesized by treatment of **2** with ethyl chloroformate, followed by reduction with LiAlH<sub>4</sub> in 41% overall yield. In order to study whether the basicity of the nitrogen atom may affect the antiviral activity, we synthesized acetamidine **17** by reaction of amine **2** with methyl acetimidate, and guanidine **18** by reaction of amine **2** with 1*H*-pyrazole-1-carboxamidine. Finally, starting from known acid **20** (Camps et al., 2001), we prepared rimantadine analog **22**, through a sequence that involved formation of ketone **21**, conversion into its oxime, and LiAlH<sub>4</sub> reduction (Fig. 4).

In a similar way, starting from the known pyrrolidine derivatives **3** and **5**, we synthesized methyl derivatives **23** and **29**, respectively, by reductive alkylation with formaldehyde and NaCNBH<sub>3</sub>. Hydrogenation of diene **23** led to the fully saturated derivative **26**. Also, the corresponding acetamidines (**24**, **27** and **30**) and guanidines (**25**, **28** and **31**), derived from **3**, **4** and **5**, respectively, were synthesized in high yields (Fig. 5).

All of the new compounds, except **18**, were fully characterized as hydrochlorides, through their spectroscopic data and elemental analyses (see Supplementary data). Compound **18** was fully characterized as its (2*R*,3*R*)-tartrate, through its spectroscopic data and high resolution mass spectrum (HRMS).

### 3.2. Inhibition of wt and Amt-insensitive A/M2 ion channels

A selection of the compounds was evaluated for inhibitory activity toward the A/M2 protein expressed in *Xenopus* oocytes, using the two-electrode voltage clamp (TEV) technique (Ma et al.,

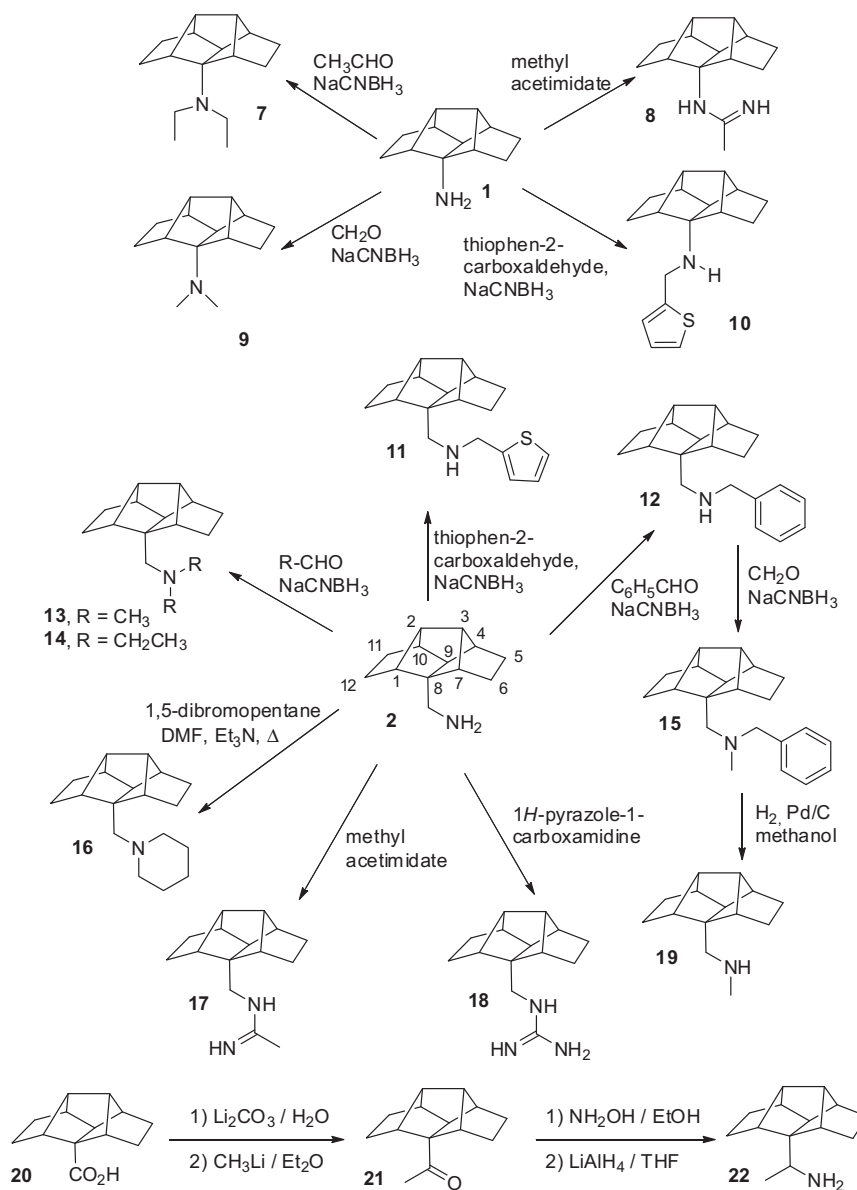


Fig. 4. Scheme for the synthesis of pentacyclo[6.4.0.0<sup>2,10</sup>.0<sup>3,7</sup>.0<sup>4,9</sup>]dodecane derivatives.

2008; Balannik et al., 2009). The compounds were initially tested at 100  $\mu\text{M}$ . Those that inhibited the wt A/M2 channel activity by more than 80% were subsequently tested in dose–response experiments, to determine their 50% inhibitory concentration ( $\text{IC}_{50}$ ). The results are given in Table 1. Amt inhibited the wt A/M2 channel with an  $\text{IC}_{50}$  of 16  $\mu\text{M}$ , and a similar value was obtained with rimantadine ( $\text{IC}_{50}$  of 11  $\mu\text{M}$ ). As previously reported, the secondary amines **3** and **5** inhibited the wt A/M2 channel with  $\text{IC}_{50}$  values similar to that of Amt ( $\text{IC}_{50}$ : 34  $\mu\text{M}$  for **3** and 24  $\mu\text{M}$  for **5**, respectively) (Duque et al., 2011). Alike Amt and rimantadine, compounds **3** and **5** were inactive against the S31N or V27A mutant forms of A/M2 (data not shown). We also determined the inhibitory activity of several of our novel compounds, i.e. the 2,2-diethylamantadines **6b** and **6c** and the pyrrolidine derivatives **26**, **29** and **30**. Unfortunately, neither of these significantly inhibited the wt, V27A or S31N A/M2 channels.

### 3.3. Antiviral activity in cell culture and structure–activity relationship

All Amt analogs synthesized were subjected to antiviral evaluation against a wide range of DNA and RNA viruses, using CPE

reduction assays in relevant cell lines. None of the compounds displayed activity against the enveloped DNA viruses herpes simplex virus (type 1 or type 2) or vaccinia virus; the enveloped RNA viruses feline coronavirus, parainfluenza-3 virus, respiratory syncytial virus, vesicular stomatitis virus, Sindbis virus or Punta Toro virus; or the non-enveloped RNA viruses Coxsackievirus B4 and Reovirus-1 (data not shown).

In our basic CPE reduction assays with influenza virus, performed in MDCK cell cultures, three virus strains were used: the A/PR/8/34 strain, an A/H1N1 virus with two Amt-resistance mutations (S31N and V27T) in the A/M2 protein; the A/HK/7/87 strain, which has a wt A/M2 protein, and the B/HK/5/72 strain. The antiviral data obtained by microscopic scoring of the virus-induced CPE were confirmed by the colorimetric MTS cell viability assay (data not shown). In parallel, the compounds were applied to uninfected MDCK cells to estimate the cytotoxicity by microscopy or MTS cell viability assay.

As shown in Table 1, only one compound, diene **3**, a secondary amine, displayed activity against both the A/H1N1 and the A/H3N2 virus (antiviral  $\text{EC}_{50}$  values of 14 and 16  $\mu\text{M}$ , respectively). For compound **3**, Amt and rimantadine, a nice correlation was seen

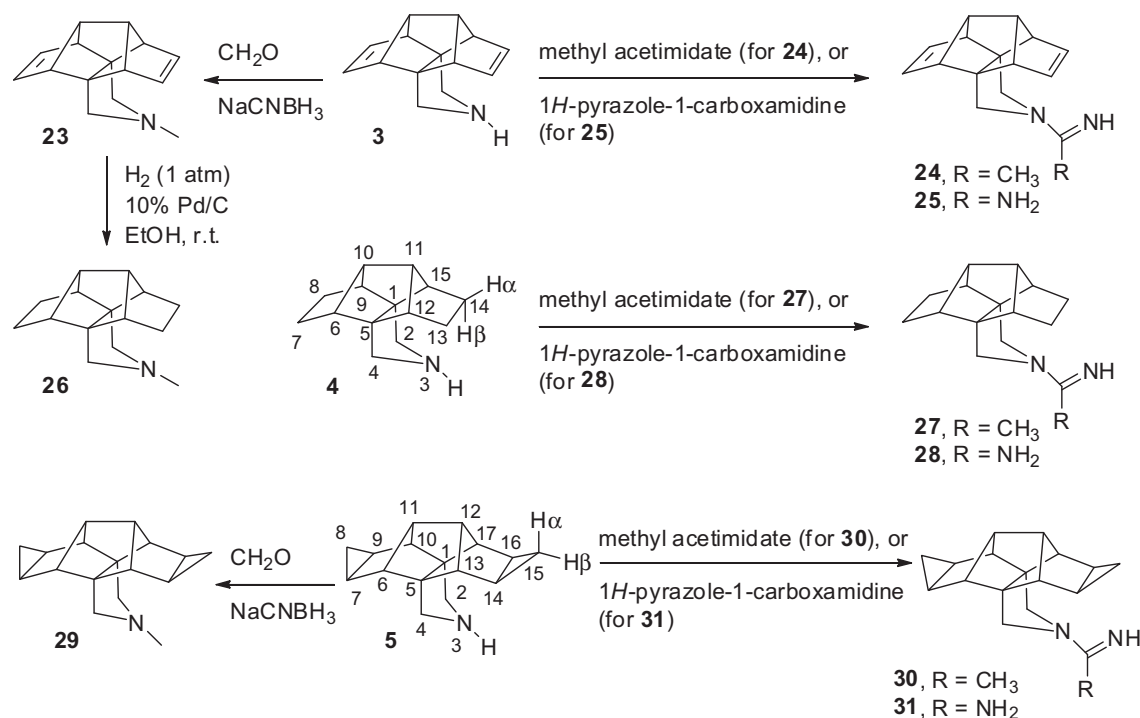


Fig. 5. Scheme for the synthesis of polycyclic pyrrolidine derivatives.

between their cell culture activities for the A/HK/7/87 virus and their  $\text{IC}_{50}$  values against A/M2 wt proton channel function (Table 1). This was, however, not the case for the bis-cyclopropanated derivative of **3**, the octacyclo compound **5**. The latter compound had quite pronounced cytotoxicity for the MDCK cells in our three-day CPE reduction assay (MCC: 22  $\mu\text{M}$  and  $\text{CC}_{50}$ : 44  $\mu\text{M}$ ), and this may have masked its potential inhibitory effect towards the A/HK/7/87 virus.

In striking contrast to the overall lack of activity against the A/H3N2 virus, several of our polycyclic amines displayed low micromolar activity against the influenza A/H1N1 virus. Many of the active compounds produced no cytotoxicity at 100  $\mu\text{M}$  (the highest concentration tested), yielding a favorable selectivity index (defined as the ratio between the cytotoxic and the antiviral concentration for the A/H1N1 virus). The compounds showing the highest potency ( $\text{EC}_{50}$  of 1  $\mu\text{M}$  or less) were two tertiary amines, **7** and the diene **23**; the bis-cyclopropanated secondary amine **5** and the guanidine **28**. As anticipated, all compounds proved to be inactive against influenza B virus (data not shown), which is known to be insensitive to Amt and rimantadine.

Analysis of the structure–activity relationship for the anti-A/H1N1 data yielded the following insights. Most pentacyclic compounds derived from primary amine **1** ( $\text{IC}_{50}$ : 10  $\mu\text{M}$ ) displayed activity against the A/H1N1 virus, with the diethyl derivative **7** being the most potent and selective one ( $\text{EC}_{50}$ : 0.8  $\mu\text{M}$ ; selectivity index >125). In contrast, among the derivatives of primary amine **2** ( $\text{EC}_{50}$ : 9.1  $\mu\text{M}$ ), only guanidine **18** ( $\text{EC}_{50}$ : 2.2  $\mu\text{M}$ ) was more potent than the parent compound. This compound **18** had a reasonable selectivity index of 9. The anti-A/H1N1 activity was reduced when substituting the “amantadine-like” structure of **1** ( $\text{EC}_{50}$ : 10  $\mu\text{M}$ ) for the “rimantadine-like” structure in **22** ( $\text{EC}_{50}$ : 22  $\mu\text{M}$ ). Of note, in going from the primary amines **1** and **2** to the more basic acetamidines **8** and **17**, complete loss of the antiviral activity was observed.

While methylation of the primary amines **1** ( $\text{EC}_{50}$ : 10  $\mu\text{M}$ ) and **2** ( $\text{EC}_{50}$ : 9  $\mu\text{M}$ ) led to less potent compounds (**9**, 19  $\mu\text{M}$ ; **19**, 21  $\mu\text{M}$ ;

**13**, >100  $\mu\text{M}$ ), for the pyrrolidine derivatives **4** and **5**, the corresponding methylated compounds (**26** and **29**, respectively) displayed similar antiviral activity with  $\text{EC}_{50}$  values in the low micromolar range. For the pyrrolidine derivative **3** ( $\text{EC}_{50}$ : 16  $\mu\text{M}$ ), the methylated derivative, **23**, was considerably more active ( $\text{EC}_{50}$ : 0.4  $\mu\text{M}$ ).

The impact of introducing the strongly basic guanidine group was less clear. While the amines **2** and **4** were less potent than their corresponding guanidines, **18** and **28**, respectively, complete loss of the antiviral activity was observed in going from amines **3** and **5** to their corresponding guanidines, **25** and **31**, respectively.

Several compounds with activity against the A/PR/8/34 (A/H1N1) strain but not the A/HK/7/87 (A/H3N2) strain were further evaluated against the A/Victoria/3/75 (A/H3N2) strain. Both these A/H3N2 strains carry a wt A/M2 protein. The selected compounds (i.e. **2–4**, **7**, **19**, **26** and **29**) were also inactive against the A/Victoria/3/75 strain ( $\text{EC}_{50}$  > 100  $\mu\text{M}$ , the highest concentration tested; data not shown). These data argue against the possibility that the inactivity of these compounds against A/H3N2 virus may have been specific for the A/HK/7/87 strain.

### 3.4. Evaluation against a broad panel of influenza A/H1N1 and A/H3N2 viruses

The two more potent compounds, tertiary amines **7** and **23**, endowed with submicromolar activity against the A/PR/8/34 (A/H1N1) strain ( $\text{EC}_{50}$ : 0.80 and 0.40  $\mu\text{M}$ , respectively), and the secondary amine **4** ( $\text{EC}_{50}$ : 2.0  $\mu\text{M}$ ), as well as three 2,2-dialkylamantadine derivatives that we recently synthesized (**6a**, **6b** and **6c**; Fig. 3) (Torres et al., 2012), were selected for evaluation against a broader panel of influenza A/H1N1 and A/H3N2 viruses. This panel contained two Amt-sensitive A/H1N1 viruses and one Amt-insensitive strain (i.e. the 2009 pandemic A/H1N1 virus) and A/X-31, a chimeric strain carrying the H3 and N2 proteins of A/Aichi/2/68 and the other proteins (including M2) from the Amt-resistant A/PR/8/34 strain. All seven influenza A virus strains used were

**Table 1**  
Inhibitory effect of different series of polycyclic amines against influenza A virus replication in MDCK cells, and proton channel function of influenza A/M2 wt protein.

| Compound                           | Nitrogen atom function | Anti-influenza virus activity in MDCK cells  |                    |                       |                                    | Activity against A/M2 wt channel <sup>b</sup> |                       |
|------------------------------------|------------------------|--|--------------------|-----------------------|------------------------------------|---|-----------------------|
|                                    |                        | Antiviral EC <sub>50</sub> <sup>a</sup> (μM) |                    | Cytotoxicity          |                                    | Inhibition at 100 μM (%)                      | IC <sub>50</sub> (μM) |
|                                    |                        | A/H1N1 (A/PR/8/34)                           | A/H3N2 (A/HK/7/87) | MCC <sup>c</sup> (μM) | CC <sub>50</sub> <sup>d</sup> (μM) |   |                       |
| <i>Derivatives of pentacycle 1</i> |                        |  |                    |                       |                                    |   |                       |
| <b>1</b>                           | –NH <sub>2</sub>       | 10   | >100               | 100                   | >100                               | 4.8 ± 2.8 <sup>e</sup>                        | ND                    |
| <b>10</b>                          | –NHR                   | 8  | >100               | 34                    | ≥20                                | ND  | ND                    |
| <b>7</b>                           | –NR <sub>2</sub>       | 0.80   | >100               | >100                  | >100                               | 0 <sup>e</sup>                                | ND                    |
| <b>9</b>                           | –NR <sub>2</sub>       | 19   | >100               | ≥100                  | >100                               | ND  | ND                    |
| <b>8</b>                           | Amidine                | >100   | >100               | 20                    | 14                                 | 9.3 ± 2.4 <sup>e</sup>                        | ND                    |
| <i>Derivatives of pentacycle 2</i> |                        |  |                    |                       |                                    |   |                       |
| <b>2</b>                           | –NH <sub>2</sub>       | 9.1  | >100               | ≥86                   | 78                                 | 13 ± 1 <sup>e</sup>                           | ND                    |
| <b>22</b>                          | –NH <sub>2</sub>       | 22   | >100               | >100                  | ≥100                               | ND  | ND                    |
| <b>11</b>                          | –NHR                   | >100   | >100               | 6                     | 30                                 | ND  | ND                    |
| <b>12</b>                          | –NHR                   | >100   | >100               | 20                    | 12                                 | ND  | ND                    |
| <b>19</b>                          | –NHR                   | 21   | >100               | >100                  | >100                               | 15 ± 2 <sup>e</sup>                           | ND                    |
| <b>13</b>                          | –NR <sub>2</sub>       | >100   | >100               | 40                    | 47                                 | ND  | ND                    |
| <b>14</b>                          | –NR <sub>2</sub>       | >100   | >100               | 30                    | 47                                 | ND  | ND                    |
| <b>15</b>                          | –NR <sub>2</sub>       | >100   | >100               | 0.1                   | 0.04                               | ND  | ND                    |
| <b>16</b>                          | –NR <sub>2</sub>       | >100   | >100               | 64                    | 150                                | ND  | ND                    |
| <b>17</b>                          | Amidine                | >100   | >100               | >100                  | >100                               | ND  | ND                    |
| <b>18</b>                          | Guanidine              | 2.2  | >100               | ≥20                   | 45                                 | ND  | ND                    |
| <i>Pirrolidine derivatives</i>     |                        |  |                    |                       |                                    |   |                       |
| <b>3</b>                           | –NH–                   | 16   | 14                 | >100                  | >100                               | 82 ± 1 <sup>e</sup>                           | 34 ± 2                |
| <b>4</b>                           | –NH–                   | 2.0  | >100               | >100                  | ≥100                               | 40 ± 1 <sup>e</sup>                           | ND                    |
| <b>5</b>                           | –NH–                   | 1.0  | >100               | 22                    | 40                                 | 86 ± 1 <sup>e</sup>                           | 24 ± 2                |
| <b>23</b>                          | –NR–                   | 0.40   | >100               | ≥100                  | ≥74                                | ND  | ND                    |
| <b>26</b>                          | –NR–                   | 2.9  | >100               | 27                    | ≥20                                | 4.1 ± 1.1                                     | ND                    |
| <b>29</b>                          | –NR–                   | 4.6  | >100               | 31                    | ≥20                                | 27 ± 1  | ND                    |
| <b>24</b>                          | Amidine                | 4.9  | >100               | 100                   | 52                                 | ND  | ND                    |
| <b>27</b>                          | Amidine                | ≤2.3   | >100               | ≥100                  | >100                               | ND  | ND                    |
| <b>30</b>                          | Amidine                | >100   | >100               | 56                    | 31                                 | 20 ± 2  | ND                    |
| <b>25</b>                          | Guanidine              | >100   | >100               | ≥20                   | >100                               | ND  | ND                    |
| <b>28</b>                          | Guanidine              | 1.3  | >100               | ≥20                   | >100                               | ND  | ND                    |
| <b>31</b>                          | Guanidine              | >100   | >100               | 69                    | ≥35                                | ND  | ND                    |
| <i>2,2-Diethylamantadines</i>      |                        |  |                    |                       |                                    |   |                       |
| <b>6a</b>                          | –NH <sub>2</sub>       | 2.0 <sup>f</sup>                             | >100               | ≥100                  | >100                               | ND  | ND                    |
| <b>6b</b>                          | –NHR                   | 4.0 <sup>f</sup>                             | >100               | ≥100                  | >100                               | 15 ± 3  | ND                    |
| <b>6c</b>                          | –NR <sub>2</sub>       | 4.0 <sup>f</sup>                             | >100               | ≥100                  | >100                               | 24 ± 1  | ND                    |
| Amantadine                         | –NH <sub>2</sub>       | 53   | 3.4                | ≥500                  | >500                               | 91 ± 2  | 16 ± 1                |
| Rimantadine                        | –NH <sub>2</sub>       | 4.6  | 0.17               | 500                   | 230                                | 91.4 ± 0.8                                    | 10.8 ± 0.7            |

ND, not determined.

<sup>a</sup> EC<sub>50</sub>: concentration producing 50% antiviral effect, as determined by microscopy of the virus-induced CPE.

<sup>b</sup> Isochronic (2 min) values for IC<sub>50</sub> are given. Data are the mean ± SEM.

<sup>c</sup> MCC: minimum cytotoxic concentration, i.e. concentration causing minimal changes in cell morphology.

<sup>d</sup> CC<sub>50</sub>: 50% cytotoxic concentration, determined by the MTS cell viability assay.

<sup>e</sup> From Duque et al. (2011).

<sup>f</sup> From Torres et al. (2012).

characterized by M gene sequencing to detect Amt-resistance mutations, and by determining their hemolysis pH (Table 2). The latter was done in the context of our finding that resistance to the polycyclic amines was associated with mutations in the HA protein, leading to an increased hemolysis pH (see below).

As shown in Table 2, the three polycyclic compounds **4**, **7** and **23** as well as the three 2,2-diethylamantadine derivatives **6a**, **6b** and **6c** had an identical spectrum for anti-influenza virus activity, showing micromolar activity against all four A/H1N1 strains, while being totally inactive against the three A/H3N2 strains.

Finally, the strong inhibitory effect against strain A/PR/8/34 was confirmed in a virus yield assay in MDCK cells (Table 3). The three polycyclic amine compounds evaluated in this assay produced a strong reduction in infectious virus titer, with EC<sub>99</sub> values (i.e. concentrations producing a 2-log<sub>10</sub> reduction in virus titer) of 3.2 μM (**4**), 1.5 μM (**7**) and 3.5 μM (**6c**). Amantadine and rimantadine were much less potent since their EC<sub>99</sub> values were 179 and 48 μM, respectively.

### 3.5. Selection and characterization of polycyclic amine-resistant virus mutants

The strict activity of our structurally diverse polycyclic amines against A/H1N1 viruses, whether containing a wt or Amt-resistant M2 protein, pointed to the viral hemagglutinin as the likely antiviral target. It has been known since many years that M2 inhibition by amantadine occurs at lower (micromolar) compound concentrations, while at higher concentrations (100 μM or more), amantadine increases the endosomal pH, thereby interfering with the low pH-induced and HA-mediated membrane fusion (Daniels et al., 1985). This explains why viruses that have been selected under amantadine in cell culture regularly contain mutations in HA that increases the fusion pH of the virus. These mutant HAs adopt their fusogenic conformation at less acidic pH, thus escaping the pH-increasing effect of amantadine. In this study, we serially passed the influenza A/PR/8/34 virus in the presence of the secondary hexacyclic amine **4** or the 2,2-diethyladamantyl tertiary amine **6c**, which were chosen because of their superior selectivity,

**Table 2**

Antiviral activity against a broader panel of influenza A/H1N1 and A/H3N2 viruses, evaluated in MDCK cells.

| Compound   | A/H1N1 subtype |              |           |                        | A/H3N2 subtype |             |                 | Cytotoxicity<br>(MCC in $\mu\text{M}$ ) <sup>a</sup> |
|--|----------------|--------------|-----------|------------------------|----------------|-------------|-----------------|--|
|  | A/PR/8/34      | A/Ned/378/05 | A/FM/1/47 | A/2009pan <sup>b</sup> | A/X-31         | A/HK/7/87   | A/Ishikawa/7/82 |  |
| Amt-resistance mutations in M2 <sup>c</sup>                          |                |              |           |                        |                |             |                 |  |
|  | V27T/S31N      | wt           | wt        | S31N                   | V27T/S31N      | wt          | wt              |  |
| Virus hemolysis pH <sup>d</sup>                                      |                |              |           |                        |                |             |                 |  |
|  | 5.0            | 5.1          | 5.2       | 5.2                    | 5.0            | 5.2         | 5.3             |  |
| Antiviral activity (EC <sub>50</sub> in $\mu\text{M}$ ) <sup>e</sup> |                |              |           |                        |                |             |                 |  |
| <b>4</b>   | 8.0 ± 2.2      | 50 ± 0       | 12 ± 3    | 75 ± 12                | >100           | >100        | >100            | >100   |
| <b>7</b>   | 1.2 ± 0.6      | 8.7 ± 3.3    | 18 ± 11   | 11 ± 6                 | >100           | >100        | >100            | >100   |
| <b>23</b>  | 0.40 ± 0.00    | 7.0 ± 0.0    | 10 ± 3    | ND                     | >100           | >100        | >100            | >100   |
| <b>6a</b>  | 1.2 ± 0.5      | 4.7 ± 1.3    | 7.0 ± 0.0 | ND                     | >100           | >100        | >100            | >100   |
| <b>6b</b>  | 5.0 ± 2.5      | 8.7 ± 0.3    | 9.3 ± 0.3 | ND                     | >100           | >100        | >100            | >100   |
| <b>6c</b>  | 0.70 ± 0.39    | 23 ± 3       | 43 ± 12   | 28 ± 8                 | >100           | >100        | >100            | ≥ 100  |
| Amantadine   | 53 ± 11        | 2.0 ± 0.0    | 5.1 ± 2.4 | 137 ± 10               | 61 ± 12        | 3.4 ± 1.7   | 11 ± 8          | 500  |
| Rimantadine  | 4.6 ± 1.8      | 0.50 ± 0.22  | 1.9 ± 1.1 | ≥ 158                  | 7.0 ± 1.7      | 0.17 ± 0.08 | 0.45 ± 0.15     | >100   |
| Oseltamivir carboxylate  | 21 ± 9         | 1.5 ± 0.8    | 16 ± 2    | ND                     | 0.11 ± 0.05    | 29 ± 5      | 3.0 ± 1.0       | >100   |
| Zanamivir  | 6.0 ± 1.3      | 1.7 ± 0.5    | 5.0 ± 1.6 | ND                     | 0.16 ± 0.05    | 1.2 ± 0.9   | 8.7 ± 3.8       | >100   |
| Ribavirin  | 8.7 ± 0.7      | 7.6 ± 1.0    | 10 ± 1    | 11 ± 1                 | 8.8 ± 0.2      | 8.6 ± 0.4   | 8.8 ± 0.3       | >100   |

ND, not determined.

<sup>a</sup> MCC: minimum cytotoxic concentration, or compound concentration producing minimal alterations in cell morphology.<sup>b</sup> A/H1N1 2009 pandemic virus strain: A/Virginia/ATCC3/2009.<sup>c</sup> For each virus strain, the entire M2 coding region was sequenced, but only the residues associated with Amt resistance (i.e. located between M2 residues 26–34) are mentioned here.<sup>d</sup> For each virus strain, the hemolysis pH was determined (defined as the pH at which 50% hemolysis occurs) (see Vanderlinden et al., 2010 for the procedure).<sup>e</sup> The EC<sub>50</sub> represents the compound concentration producing 50% inhibition of virus replication, as determined by microscopic scoring of the CPE.

making it possible to apply compound concentrations as high as 150  $\mu\text{M}$ . These two compounds are each representative of their structural series, with **4** being a secondary amine and **6c** being a tertiary amine. A control condition in which the virus was passed in the absence of test compound was included, to identify which HA mutations appear as the virus, produced in eggs, is adapted to cell culture.

As summarized in Table 4, five residue changes (using H1 numbering as in Gamblin et al., 2004) were detected in the HA1 or HA2 polypeptide parts of the HA protein. Sequence analysis on our parent A/PR/8/34 allantoic stock showed that, at this stage, the virus was still homogeneous, since no double peaks were observed. A wide survey of published sequences of the A/PR/8/34 HA (Bao et al., 2008) (<http://www.ncbi.nlm.nih.gov/genomes/FLU/FLU.html>) demonstrated that for two of the five changes (i.e. HA<sub>1</sub>-P186S and HA<sub>1</sub>-I324T), the observed variation has been reported, suggesting that these changes naturally occur without selective pressure. In the virus passed in the absence of compound, an HA<sub>2</sub>-I10V substitution became apparent after two passages, and this mutant was the only one remaining after eight passages, indicating that it results from cell culture adaptation of the A/PR/8/34 virus. The two remaining changes were clearly selected by our polycyclic amines: HA<sub>1</sub>-A13T, which was present in the #8 passage selected under compound **4**, and HA<sub>2</sub>-F3L, which was already apparent after two passages with **6c**. The virus selected under **4** also contained the HA<sub>1</sub>-P186S and HA<sub>1</sub>-I324T changes, which appeared early on and of which the relevance is not clear since, as explained above, these may well be polymorphic changes.

Our sequencing data strongly argued for a role of the HA protein in the antiviral mode of action of **4** and **6c**, and, most likely, the other polycyclic amines studied here. A parallel can be seen with the HA changes obtained under Amt, which result in an increased fusion pH, thus rendering the virus resistant to the pH-increasing effect of Amt (Daniels et al., 1985). We therefore determined the hemolysis pH, defined as the pH at which 50% hemolysis occurs when virus attached to erythrocytes is exposed to different acidic buffers (Vanderlinden et al., 2010). The hemolysis pH of our parent

allantoic A/PR/8/34 virus was quite low (4.9; Table 4). This value was increased (to 5.2) in the cell culture-adapted virus containing the HA<sub>2</sub>-I10V change. The mutant viruses obtained under **4** or **6c** had a considerably higher hemolysis pH of 5.7 and 5.5, respectively, indicating that acquisition of a less stable HA that is able of fusing at higher pH, confers resistance to the polycyclic amines.

Antiviral evaluation of the #8 passages, with the parent allantoic stock tested in parallel, demonstrated that the fusion mutants obtained under **4** and **6c** were fully resistant to both polycyclic amines, and cross-resistant to Amt and rimantadine, whereas their sensitivity to ribavirin was the same as that of the allantoic virus (Table 5). The #8 virus obtained in the absence of compound, which had an intermediate hemolysis pH of 5.2, was less sensitive to all four Amt derivatives, the factor increase in antiviral EC<sub>50</sub> (compared to the parent allantoic virus) being 11 (compound **4**); 4 (compound **6c** and Amt) and >27 (rimantadine). Thus, a correlation was seen between the viral hemolysis pH and the antiviral sensitivity to each of the four amines.

#### 4. Discussion

After endocytic uptake of the influenza virus into the host cell, the viral genome segments must be released into the cytoplasm and transported to the nucleus to initiate RNA transcription and replication (Cross et al., 2001a). This endosomal escape of the virus critically depends on the activity of two viral proteins which are both activated at the low endosomal pH: the M2 proton channel, required for uncoating of the viral ribonucleoproteins, and the HA protein, which upon acidification adopts a fusogenic conformation to cause fusion of the endosomal and viral membranes and formation of a fusion pore (Cross et al., 2001a). Therefore, dually acting polycyclic amines which combine blockade of the M2 channel with an inhibitory effect on HA refolding, appear highly attractive. This dual approach could also, at least in theory, increase the barrier for selecting adamantane resistance (Scholtissek et al., 1998). Optimized adamantane derivatives might be able to exert this dual pharmacological effect, provided that both the M2 and

**Table 3**

Activity of some polycyclic amine compounds against influenza virus A/PR/8/34 in a virus yield assay in MDCK cells.

| Compound    | EC <sub>99</sub> (μM) <sup>a</sup> |
|-------------|------------------------------------|
| <b>7</b>    | 1.5 ± 0.4                          |
| <b>4</b>    | 3.2 ± 0.9                          |
| <b>6c</b>   | 3.5 ± 0.9                          |
| Amantadine  | 179 ± 53                           |
| Rimantadine | 48 ± 5                             |
| Ribavirin   | 11 ± 1                             |

Values shown are the mean ± SEM (*n* = 2).

<sup>a</sup> EC<sub>99</sub>: compound concentration producing a 2-log<sub>10</sub> reduction in virus yield in MDCK cells. Virus released in the supernatant at 72 h p.i. was quantified by determining the infectious virus titer, using the CCID<sub>50</sub> method. Virus strain: A/H1N1; strain A/PR/8/34.

HA inhibition occur at similar and relevant compound concentrations. For comparison, the M2 blocking effect of Amt is achieved at micromolar concentrations, whereas its increasing effect on the endosomal pH requires much higher concentrations (i.e. in the range of 100 μM). These high Amt concentrations cannot be achieved *in vivo* with the standard Amt drug regimens, since the reported plasma concentration values for Amt are in the range of 2 μM (Hayden et al., 1985). Hence, to potentially exploit the effect of adamantane derivatives on HA refolding, novel analogues with a more potent activity would be required.

During the past years, our group has synthesized different series of polycyclic amines, the first aim being to improve the inhibitory effect towards M2 and/or achieve activity against Amt-resistant M2 proton channels (Camps et al., 2008; Duque et al., 2011; Torres et al., 2012). Upon evaluation of our compounds in influenza virus-infected cells, we noticed that several displayed micromolar activity against the A/PR/8/34 virus, an A/H1N1 virus carrying two characteristic Amt resistance mutations in its M2 protein, while being inactive against the A/HK/7/87 virus, which contains a wt A/M2. In the present report, this particular subtype dependency was investigated in more detail, by using different series of polycyclic amines (including a newly synthesized series of hexacyclo and octacyclo compounds) and a broad panel of A/H1N1 and A/H3N2 viruses. In CPE reduction assays, low micromolar activity (EC<sub>50</sub> < 10 μM) against the A/PR/8/34 virus was observed with several compounds, the most noticeable being: the pyrrolidine derivatives **4**, **5**, **23**, **24** and **26–29**; the primary amine **2**; the secondary

amine **10**; the tertiary amine **7**; and the guanidine **18**. The most potent derivative, diene **23**, had an EC<sub>50</sub> value of 0.4 μM and a selectivity index of 250. Another intriguing compound, the hexacyclodiene **3**, was active against both the A/PR/8/34 and A/HK/7/87 strains, and, moreover, inhibited wt A/M2 channel function with a similar IC<sub>50</sub> value as amantadine. This compound may represent a lead for dually acting polycyclic amines. To further increase the antiviral potency, the synthesis of compound **3** derivatives should be considered.

We hypothesized that the potent activity of our polycyclic amines against the Amt-resistant A/PR/8/34 virus most likely results from interference with HA-mediated fusion, alike seen with high concentrations of Amt. A/PR/8/34 virus mutants obtained after serial passaging in the presence of the secondary amine **4** or the tertiary amine **6c** indeed contained mutations in the HA protein that considerably increased the pH of hemolysis, meaning that these mutant HAs adopt their fusogenic conformation at higher pH. In Fig. 6, the five residues that were subject to mutation in our passaged viruses were located in the published crystal structure of the A/PR/8/34 HA (Gamblin et al., 2004). Three of these changes [HA<sub>1</sub>-P186S, located in the globular head, and HA<sub>1</sub>-I324T and HA<sub>2</sub>-I10V, both located in the HA stem near the fusion peptide] seemed to be polymorphic and/or related to cell culture adaptation (Lin et al., 1997) and, hence, were considered irrelevant in the context of our polycyclic amines. The HA<sub>2</sub>-F3L residue change selected under **6c** was previously identified by Daniels et al. (1985) in an Amt-resistant avian A/H7N1 virus (Weybridge strain), which manifested an increase in hemolysis pH of 0.4 pH units. The HA<sub>2</sub>-F3L mutation was also reported by Plotch et al. (1999), who selected a virus for resistance to the small molecule fusion inhibitor CL-61917, starting from an Amt-resistant A/FM/47 virus. The increased fusion pH of the HA<sub>2</sub>-F3L mutant virus is not unexpected, since this residue lies in the hydrophobic fusion peptide of HA. It has been reported that introduction of less hydrophobic residues into the fusion peptide results in an increased fusion pH (Cross et al., 2001b). The side chains of HA<sub>2</sub>-Phe3, located in the heart of the trimeric HA stem, make several hydrophobic contacts among each other and with surrounding residues. Replacing these Phe-3 residues by smaller leucines probably decreases the hydrophobic interactions with surrounding residues, which may promote easier release of the fusion peptide from its binding position, thus explaining the increased fusion pH. Regarding the HA<sub>1</sub>-A13T substitution selected under compound **4**, the impact of this residue change is less obvious. In the neutral pH structure of the A/PR/8/34 HA protein

**Table 4**

Amino acid substitutions in the viral HA after passaging with **4** or **6c**, and their impact on the pH of hemolysis.

| Virus <sup>a</sup>     | Amino acid residue <sup>b</sup> |                      |                      |                    |                     | Hemolysis pH <sup>d</sup> |
|------------------------|---------------------------------|----------------------|----------------------|--------------------|---------------------|---------------------------|
|                        | HA <sub>1</sub> -13             | HA <sub>1</sub> -186 | HA <sub>1</sub> -324 | HA <sub>2</sub> -3 | HA <sub>2</sub> -10 |                           |
| Published <sup>c</sup> | Ala                             | Pro/Ser              | Ile/Thr              | Phe                | Ile                 |                           |
| Parent allantois       | Ala                             | Pro                  | Ile                  | Phe                | Ile                 | 4.9 ± 0.0                 |
| No cpd #1              | Ala                             | Pro/Ser              | Ile                  | Phe                | Ile                 |                           |
| No cpd #2              | Ala                             | Pro/Ser              | Ile                  | Phe                | Ile/Val             |                           |
| No cpd cl 1-2-3        | Ala                             | Pro                  | Ile                  | Phe                | Val                 | 5.2 ± 0.0                 |
| <b>4</b> #1            | Ala                             | Ser                  | Ile/Thr              | Phe                | Ile                 |                           |
| <b>4</b> #2            | Ala                             | Ser                  | Thr                  | Phe                | Ile                 |                           |
| <b>4</b> #8 cl 1-2-3   | Thr                             | Ser                  | Thr                  | Phe                | Ile                 | 5.7 ± 0.1                 |
| <b>6c</b> #1           | Ala                             | Pro                  | Ile                  | Phe                | Val                 |                           |
| <b>6c</b> #2           | Ala                             | Pro                  | Ile                  | Leu                | Val                 |                           |
| <b>6c</b> #8 cl 1-2-3  | Ala                             | Pro                  | Ile                  | Leu                | Val                 | 5.5 ± 0.0                 |

Values shown are the mean ± SEM (*n* = 2).

<sup>a</sup> Influenza virus (A/H1N1; strain A/PR/8/34) was passed in MDCK cells in the presence of **4**, **6c** or no compound, and passages #1; #2 and #8 were subjected to HA sequence analysis. For passage #8, individual virus clones (cl1, cl2 and cl3) were first isolated by plaque purification.

<sup>b</sup> Amino acid residues at the indicated positions in the HA<sub>1</sub> or HA<sub>2</sub> polypeptides of the HA protein. HA numbering as in Gamblin et al. (2004).

<sup>c</sup> Published sequences for A/PR/8/34 hemagglutinin (GI accession numbers: 89779321, 392340000 and 323696012).

<sup>d</sup> To prepare concentrated stocks for determining the hemolysis pH (Vanderlinden et al., 2010), the isolated virus clones were expanded by one passage in eggs.

**Table 5**  
Antiviral resistance profile of the influenza virus clones obtained after selection with **4** or **6c**.

| Virus <sup>a</sup>            | Hemolysis pH <sup>b</sup> | Antiviral activity (EC <sub>50</sub> in μM) <sup>c</sup> |           |            |             |           |
|-------------------------------|---------------------------|--|-----------|------------|-------------|-----------|
|                               |                           | <b>4</b>   | <b>6c</b> | Amantadine | Rimantadine | Ribavirin |
| Parent allantois <sup>d</sup> | 4.9 ± 0.0                 | 1.6 ± 0.6  | 1.0 ± 0.3 | 67 ± 8     | 3.7 ± 2.7   | 11 ± 5    |
| No cpd #8 cl3                 | 5.2 ± 0.0                 | 18 ± 8   | 4.5 ± 1.9 | 70 ± 30    | >100        | 15 ± 5    |
| <b>4</b> #8 cl3               | 5.7 ± 0.1                 | >100   | >100      | >250       | >100        | 26 ± 4    |
| <b>6c</b> #8 cl3              | 5.5 ± 0.0                 | >100   | >100      | >250       | >100        | 24 ± 3    |

Data shown are the mean ± SEM (n = 2).

<sup>a,b</sup> See legend to Table 4.

<sup>c</sup> EC<sub>50</sub>: compound concentration producing 50% inhibition of virus-induced CPE.

<sup>d</sup> Parent A/PR/8/34 allantois stock, used for selection of the virus clones in the presence of **4** or **6c**, or in the absence of compound.

(Fig. 6), this Ala-13 residue in HA1 lies adjacent to Tyr-11 (H1 numbering; Gamblin et al., 2004), which is reported to directly interact with the fusion peptide *via* formation of two hydrogen bonds (i.e. with HA<sub>2</sub>-Ala7 and HA<sub>2</sub>-Ile10) (Thoennes et al., 2008). The corresponding residue in H3 HA is His-17 (H3 numbering), which requires a water molecule to interact with the fusion peptide and, in contrast to tyrosine, is protonated at fusion pH. The critical role of this residue in triggering membrane fusion explains why Tyr-11 is conserved in all group-1 HAs (including H1 HA), whereas all group-2 HAs (including H3 HA) contain His-17 at the corresponding position (Thoennes et al., 2008). The importance of this HA region is consistent with our observation that the HA<sub>1</sub>-A13T substitution drastically reduces the stability of the HA, resulting in a hemolysis pH as high as 5.7. One explanation may be that a hydroxyl-containing Thr residue at position 13 may disturb the hydrogen bonding between Tyr-11 and the fusion peptide.

The fact that the polycyclic amines select for A/H1N1 escape mutants with increased fusion pH indicates that these compounds interfere with the HA-mediated fusion process. One potential mode of action, i.e. direct binding of the polycyclic amine compound to the prefusogenic HA protein, thereby preventing its refolding at low pH, was excluded in a hemolysis inhibition experiment with the A/PR/8/34 virus. We previously used the hemolysis assay to identify a small molecule fusion inhibitor of A/H3N2 viruses that acts by binding to a hydrophobic pocket in the prefusogenic HA protein (Vanderlinden et al., 2010). None of the three polycyclic amines tested (**4**, **7** and **6c**) inhibited the low pH-induced hemolysis by A/PR/8/34 at 100 μM (data not shown). In addition, the compounds did not produce any effect in a hemagglutination inhibition assay. These data argue against a direct binding interaction between the polycyclic amines and the HA regions involved in receptor binding or membrane fusion. Thus, in analogy to Amt, it is probable that the polycyclic amines act by causing a slight increase in the endosomal pH. Whereas this pH effect of Amt is only seen at ~100 μM concentrations, our compounds act at ~50-fold lower concentrations. This mode of action explains why, within the panel of A/H1N1 strains tested, a correlation was seen between the antiviral EC<sub>50</sub> values and the viral hemolysis pH (Table 2). Also, the markedly increased hemolysis pH of the A/PR/8/34 mutants resistant to the polycyclic amines means that these mutant HAs are able to fuse at conditions of higher endosomal pH, induced by the amine compounds. To try to provide direct evidence for this effect on endosomal pH, we performed the acridine orange assay with confocal microscopy visualization. This acidotropic dye becomes protonated and sequestered inside the acidic endosomes, giving a shift from green to red fluorescence. The lysosomal red fluorescence was completely inhibited by the V-ATPase inhibitor bafilomycin A1, whereas the condition receiving chloroquine showed a decrease in lysosomal pH and a shift to yellow fluorescence (data not shown, but similar to those reported by Vanderlinden et al., 2012). In contrast, neither of the polycyclic amines tested, i.e. amantadine at 500 μM, or compounds

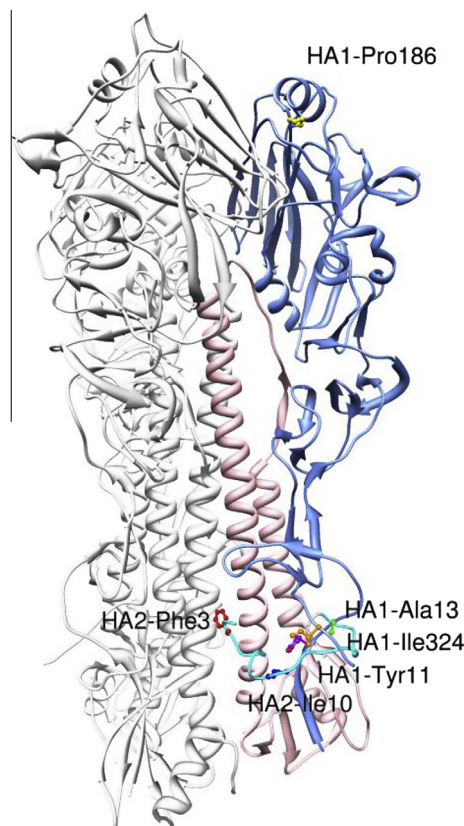


**Fig. 6.** Location of the observed residue changes in the A/PR/8/34 HA protein (pdb entry 1RU7; Gamblin et al., 2004; residue numbering taken from this reference) [Figure created using Chimera (Pettersen et al., 2004)]. One monomer of the HA trimer is colored (in blue: HA<sub>1</sub> and in pink: HA<sub>2</sub>), and the other two monomers are in light grey. The fusion peptide (residues 1–20 at the N-terminus of HA<sub>2</sub>) is in cyan. The side chains of the relevant residues are labeled as follows: HA<sub>1</sub>-Ala13, green; HA<sub>1</sub>-Pro186, yellow; HA<sub>1</sub>-Ile324, orange; HA<sub>2</sub>-Phe3, red; and HA<sub>2</sub>-Ile10, blue. The residue marked in purple is the group-1 specific HA<sub>1</sub>-Tyr11, which directly interact with the fusion peptide *via* formation of two hydrogen bonds (Thoennes et al., 2008). Except for HA<sub>1</sub>-Pro186 (located in the globular head of HA), all other marked residues are lying close to or within the fusion peptide. Changes at these positions were observed after virus passaging in cell culture in the presence of compound **4** or **6c** or in the absence of compound, and were associated with an increased pH of hemolysis. (For interpretation of the references to colour in this figure legend, the reader is referred to the web version of this article.)

**4**, **7** or **6c** (at 100 μM) changed the acridine orange staining pattern, as compared to untreated cells (data not shown). It thus appears that the effect of these amine compounds on the endosomal pH is too subtle to be detected with the acridine orange assay, in agreement with previous data reported for amantadine (Natale and McCullough, 1998).

A striking observation is that the antiviral sensitivity to the polycyclic amines is not merely determined by the viral fusion pH, since the HA subtype (i.e. H1 or H3) acts as the real discriminating factor. The most convincing evidence comes from our result that the A/PR/8/34 (A/H1N1) and A/X-31 (A/H3N2) strains display opposite sensitivity to our polycyclic amines, despite having a similarly low hemolysis pH of 5.0. It thus appears that the A/PR/8/34 HA has some feature which makes it more susceptible to a slight increase in the endosomal pH. Some parallel may be seen with the reports that the A/PR/8/34 virus is particularly sensitive to inactivation at low pH. Korte et al. (1999) demonstrated that the fusion activity of A/PR/8/34 virus was rapidly lost when the virus was preincubated at pH 5.4. For A/X-31 virus, this inactivation required a longer preincubation time and a lower pH of 5.0. These authors further showed that, at pH 5.4, the A/PR/8/34 HA displays a higher exposure of hydrophobic residues compared to A/X-31 HA, which is relevant for the initiation of membrane fusion. The fast inactivation of A/PR/8/34 HA at low pH was proposed to be related to two characteristic Glu residues that are lying close to each other in the globular head of the HA protein, causing electrostatic repulsion and a weaker trimeric stability (Rachakonda et al., 2007). An alternative explanation for the H1-specific antiviral activity of our polycyclic amines may be that some H1 HAs (such as that of the 1918 virus or the A/PR/8/34 strain) possess a second cluster of basic (particularly histidine) residues adjacent to the vestigial esterase domain (Stevens et al., 2004). A second basic patch was also found in the 2009 pandemic H1 HA (Zhang et al., 2010b), but not in other HAs, such as H3 HA (Stevens et al., 2004). It was suggested that this second basic patch creates extra electrostatic repulsions when the HA is exposed to acidic pH. Since a second cluster of basic residues is also present in the HA of some avian influenza A/H5N1 viruses (Stevens et al., 2006), it would be relevant to investigate whether these viruses are sensitive to our polycyclic amines. Unfortunately, due to biosafety constraints, these experiments could not be performed in our laboratory. With regard to the 2009 pandemic A/H1N1 virus, this virus proved to be inhibited by our polycyclic amines, although the antiviral concentrations were higher for this virus compared to those noted for A/PR/8/34, which is consistent with our finding that the latter strain has the lowest hemolysis pH of all A/H1N1 strains examined here. To our knowledge, we are the first to provide experimental evidence suggesting that, compared to other influenza viruses, A/H1N1 viruses and in particular A/PR/8/34, are more sensitive to subtle alterations in the endosomal pH, such as caused by the polycyclic amine compounds.

## Acknowledgments

MDD, ET, PC and SV thank the Spanish Ministerio de Ciencia e Innovación (FPU fellowship to MDD and ET; PC and SV: grant CTQ2011-22433) and the Generalitat de Catalunya (PC and SV: Project 2005-SGR-00180) for financial support. LN and EV acknowledge the financial support from the Geconcerteerde Onderzoeksacties (GOA/10/014), and the dedicated technical assistance from W. van Dam, S. Stevens and L. Persoons.

## Appendix A. Supplementary data

Supplementary data associated with this article can be found, in the online version, at <http://dx.doi.org/10.1016/j.antiviral.2013.06.006>.

## References

- Alves Galvão, M.G., Rocha Crispino Santos, M.A., Alves da Cunha, A.J., 2012. Amantadine and rimantadine for influenza A in children and the elderly. *Cochrane Database Syst. Rev.*, CD002745.
- Auger, D.J., Robl, J.A., Betebenner, D.A., Magnin, D.R., Khanna, A., Robertson, J.G., Wang, A., Simpkins, L.M., Taunk, P., Huang, Q., Han, S.P., Abboa-Offei, B., Cap, M., Xin, L., Tao, L., Tozzo, E., Welzel, G.E., Egan, D.M., Marcinkeviciene, J., Chang, S.Y., Biller, S.A., Kirby, M.S., Parker, R.A., Hamann, L.G., 2005. Discovery and preclinical profile of saxagliptin (BMS-477118): a highly potent, long-acting, orally active dipeptidyl peptidase IV inhibitor for the treatment of type 2 diabetes. *J. Med. Chem.* 48, 5025–5037.
- Balannik, V., Wang, J., Ohigashi, Y., Jing, X., Magavern, E., Lamb, R.A., DeGrado, W.F., Pinto, L.H., 2009. Design and pharmacological characterization of inhibitors of amantadine-resistant mutants of the M2 ion channel of influenza A virus. *Biochemistry* 48, 11872–11882.
- Bao, Y., Bolotov, P., Dervovoy, D., Kiryutin, B., Zaslavsky, L., Tatusova, T., Ostell, J., Lipman, D., 2008. The influenza virus resource at the National Center for Biotechnology Information. *J. Virol.* 82, 596–601.
- Bright, R.A., Medina, M.J., Xu, X., Pérez-Orozco, G., Wallis, T.R., Davis, X.M., Povinelli, L., Cox, N.J., Klimov, A.I., 2005. Incidence of adamantane resistance among influenza A (H3N2) viruses isolated worldwide from 1994 to 2005: a cause for concern. *Lancet* 366, 1175–1181.
- Bright, R.A., Shay, D.K., Shu, B., Cox, N.J., Klimov, A.I., 2006. Adamantane resistance among influenza A viruses isolated early during the 2005–2006 influenza season in the United States. *Jama* 295, 891–894.
- Cady, S.D., Luo, W., Hu, F., Hong, M., 2009. Structure and function of the influenza A M2 proton channel. *Biochemistry* 48, 7356–7364.
- Cady, S.D., Schmidt-Rohr, K., Wang, J., Soto, C.S., DeGrado, W.F., Hong, M., 2010. Structure of the amantadine binding site of influenza M2 proton channels in lipid bilayers. *Nature* 463, 689–692.
- Cady, S.D., Wang, J., Wu, Y., DeGrado, W.F., Hong, M., 2011. Specific binding of adamantane drugs and direction of their polar amines in the pore of the influenza M2 transmembrane domain in lipid bilayers and dodecylphosphocholine micelles determined by NMR spectroscopy. *J. Am. Chem. Soc.* 133, 4274–4284.
- Camps, P., Lukach, A.E., Rossi, R.A., 2001. Synthesis of several halobisnoradamantane derivatives and their reactivity through the S<sub>RN1</sub> mechanism. *J. Org. Chem.* 66, 5366–5373.
- Camps, P., Duque, M.D., Vázquez, S., Naesens, L., De Clercq, E., Sureda, F.S., López-Querol, M., Camins, A., Pallàs, M., Prathalingam, S.R., Kelly, J.M., Romero, V., Ivorra, D., Cortés, D., 2008. Synthesis and pharmacological evaluation of several ring-contracted amantadine analogs. *Bioorg. Med. Chem.* 16, 9925–9936.
- Cross, K.J., Burleigh, L.M., Steinhauer, D.A., 2001a. Mechanisms of cell entry by influenza virus. *Exp. Rev. Mol. Med.* 3, 1–18.
- Cross, K.J., Wharton, S.A., Skehel, J.J., Wiley, D.C., Steinhauer, D.A., 2001b. Studies on influenza haemagglutinin fusion peptide mutants generated by reverse genetics. *EMBO J.* 20, 4432–4442.
- Daniels, R.S., Downie, J.C., Hay, A.J., Knossow, M., Skehel, J.J., Wang, M.L., Wiley, D.C., 1985. Fusion mutants of the influenza virus haemagglutinin glycoprotein. *Cell* 40, 431–439.
- Duque, M.D., Ma, C., Torres, E., Wang, J., Naesens, L., Juárez-Jiménez, J., Camps, P., Luque, F.J., DeGrado, W.F., Lamb, R.A., Pinto, L.H., Vázquez, S., 2011. Exploring the size limit of templates for inhibitors of the M2 ion channel of influenza A virus. *J. Med. Chem.* 54, 2646–2657.
- Fiore, A.E., Fry, A., Shay, D., Gubareva, L., Bresee, J.S., Uyeki, T.M., 2011. Antiviral agents for the treatment and chemoprophylaxis of influenza – recommendations of the Advisory Committee on Immunization Practices (ACIP). *MMWR Recomm. Rep.* 60, 1–24.
- Gamblin, S.J., Haire, L.F., Russell, R.J., Stevens, D.J., Xiao, B., Ha, Y., Vasisht, N., Steinhauer, D.A., Daniels, R.S., Elliot, A., Wiley, D.C., Skehel, J.J., 2004. The structure and receptor binding properties of the 1918 influenza haemagglutinin. *Science* 303, 1838–1842.
- Hay, A.J., Wolstenholme, A.J., Skehel, J.J., Smith, M.H., 1985. The molecular basis of the specific anti-influenza action of amantadine. *EMBO J.* 4, 3021–3024.
- Hayden, F.G., Minocha, A., Spyker, D.A., Hoffman, H.E., 1985. Comparative single-dose pharmacokinetics of amantadine hydrochloride and rimantadine hydrochloride in young and elderly adults. *Antimicrob. Agents Chemother.* 28, 216–221.
- Hoffmann, E., Stech, J., Guan, Y., Webster, R.G., Pérez, D.R., 2001. Universal primer set for the full-length amplification of all influenza A viruses. *Arch. Virol.* 146, 2275–2289.
- Hong, M., DeGrado, W.F., 2012. Structural basis for proton conduction and inhibition by the influenza M2 protein. *Protein Sci.* 21, 1620–1633.
- Hu, F., Luo, W., Hong, M., 2010. Mechanisms of proton conduction and gating in influenza M2 proton channels from solid-state NMR. *Science* 330, 505–508.
- Hubsher, G., Haider, M., Okun, M.S., 2012. Amantadine: the journey from fighting flu to treating Parkinson disease. *Neurology* 78, 1096–1099.
- Jefferson, T., Demicheli, V., Di Pietrantonj, C., Rivetti, D., 2006. Amantadine and rimantadine for influenza A in adults. *Cochrane Database Syst. Rev.*, CD001169.
- Korte, T., Ludwig, K., Booy, F.P., Blumenthal, R., Herrmann, A., 1999. Conformational intermediates and fusion activity of influenza virus haemagglutinin. *J. Virol.* 73, 4567–4574.
- Lamoureux, G., Artavia, G., 2010. Use of the adamantane structure in medicinal chemistry. *Curr. Med. Chem.* 17, 2967–2978.

- Lin, Y.P., Wharton, S.A., Martín, J., Skehel, J.J., Wiley, D.C., Steinhauer, D.A., 1997. Adaptation of egg-grown and transfectant influenza viruses for growth in mammalian cells: selection of hemagglutinin mutants with elevated pH of membrane fusion. *Virology* 233, 402–410.
- Lipton, S.A., 2006. Paradigm shift in neuroprotection by NMDA receptor blockade: memantine and beyond. *Nat. Rev. Drug Discov.* 5, 160–170.
- Liu, J., Obando, D., Liao, V., Lifa, T., Codd, R., 2011. The many faces of the adamantyl group in drug design. *Eur. J. Med. Chem.* 46, 1949–1963.
- Ma, C., Soto, C.S., Ohigashi, Y., Taylor, A., Bournas, V., Glawe, B., Udo, M.K., DeGrado, W.F., Lamb, R.A., Pinto, L.H., 2008. Identification of the pore-lining residues of the M2 ion channel protein of influenza B virus. *J. Biol. Chem.* 283, 15921–15931.
- Naesens, L., Vanderlinden, E., Roth, E., Jeko, J., Andrei, G., Snoeck, R., Pannecouque, C., Illyes, E., Batta, G., Herczegh, P., Sztaricskai, F., 2009. Anti-influenza virus activity and structure-activity relationship of aglycoristocetin derivatives with cyclobutenedione carrying hydrophobic chains. *Antiviral Res.* 82, 89–94.
- Natale, V.A., McCullough, K.C., 1998. Macrophage cytoplasmic vesicle pH gradients and vacuolar H<sup>+</sup>-ATPase activities relative to virus infection. *J. Leukoc. Biol.* 64, 302–310.
- Pettersen, E.F., Goddard, T.D., Huang, C.C., Couch, G.S., Greenblatt, D.M., Meng, E.C., Ferrin, T.E., 2004. UCSF Chimera – a visualization system for exploratory research and analysis. *J. Comput. Chem.* 25, 1605–1612.
- Piérard, G.E., Piérard-Franchimont, C., Paquet, P., Quatresooz, P., 2009. Spotlight on adapalene. *Expert Opin. Drug Metab. Toxicol.* 5, 1565–1575.
- Pinto, L.H., Lamb, R.A., 2006. The M2 proton channels of influenza A and B viruses. *J. Biol. Chem.* 281, 8997–9000.
- Plotch, S.J., O'Hara, B., Morin, J., Palant, O., LaRoque, J., Bloom, J.D., Lang Jr., S.A., DiGrandi, M.J., Bradley, M., Nilakantan, R., Gluzman, Y., 1999. Inhibition of influenza A virus replication by compounds interfering with the fusogenic function of the viral hemagglutinin. *J. Virol.* 73, 140–151.
- Rachakonda, P.S., Veit, M., Korte, T., Ludwig, K., Böttcher, C., Huang, Q., Schmidt, M.F., Herrmann, A., 2007. The relevance of salt bridges for the stability of the influenza virus hemagglutinin. *FASEB J.* 21, 995–1002.
- Reed, L.J., Muench, H., 1938. A simple method of estimating fifty percent endpoints. *Am. J. Epidemiol.* 27, 493–497.
- Rosenberg, M.R., Casarotto, M.G., 2010. Coexistence of two adamantane binding sites in the influenza A M2 ion channel. *Proc. Natl. Acad. Sci. USA* 107, 13866–13871.
- Rossman, J.S., Lamb, R.A., 2011. Influenza virus assembly and budding. *Virology* 411, 229–236.
- Scholtissek, C., Quack, G., Klenk, H.D., Webster, R.G., 1998. How to overcome resistance of influenza A viruses against adamantane derivatives. *Antiviral Res.* 37, 83–95.
- Sharma, M., Yi, M., Dong, H., Qin, H., Peterson, E., Busath, D.D., Zhou, H.-X., Cross, T.A., 2010. Insight into the mechanisms of the influenza A proton channel from a structure in a lipid bilayer. *Science* 330, 509–512.
- Smith, N.M., Bresee, J.S., Shay, D., Uyeki, T.M., Cox, N.J., Strikas, R.A., 2006. Prevention and control of influenza – recommendations of the Advisory Committee on Immunization Practices (ACIP). *MMWR Recomm. Rep.* 55, 1–42.
- Stevens, J., Corper, A.L., Basler, C.F., Taubenberger, J.K., Palese, P., Wilson, I.A., 2004. Structure of the uncleaved human H1 hemagglutinin from the extinct 1918 influenza virus. *Science* 303, 1866–1870.
- Stevens, J., Blixt, O., Tumpey, T.M., Taubenberger, J.K., Paulson, J.C., Wilson, I.A., 2006. Structure and receptor specificity of the hemagglutinin from an H5N1 influenza virus. *Science* 312, 404–410.
- Stouffer, A.L., Acharya, R., Salom, D., Levine, A.S., Di Costanzo, L., Soto, C.S., Tereshko, V., Nanda, V., Stayrook, S., DeGrado, W.F., 2008. Structural basis for the function and inhibition of an influenza virus proton channel. *Nature* 451, 596–599.
- Thoennes, S., Li, Z.N., Lee, B.J., Langley, W.A., Skehel, J.J., Russell, R.J., Steinhauer, D.A., 2008. Analysis of residues near the fusion peptide in the influenza hemagglutinin structure for roles in triggering membrane fusion. *Virology* 370, 403–414.
- Torres, E., Vanderlinden, E., Fernández, R., Miquet, S., Font-Bardia, M., Naesens, L., Vázquez, S., 2012. Synthesis and anti-influenza activity of 2,2-dialkylamantadines and related compounds. *ACS Med. Chem. Lett.* 3, 1065–1069.
- Vanderlinden, E., Göktas, F., Cesur, Z., Froeyen, M., Reed, M.L., Russell, C.J., Cesur, N., Naesens, L., 2010. Novel inhibitors of influenza virus fusion: structure-activity relationship and interaction with the viral hemagglutinin. *J. Virol.* 84, 4277–4288.
- Vanderlinden, E., Vanstreels, E., Boons, E., ter Veer, W., Huckriede, A., Daelemans, D., Van Lommel, A., Röth, E., Sztaricskai, F., Herczegh, P., Naesens, L., 2012. Intracytoplasmic trapping of influenza virus by a lipophilic derivative of aglycoristocetin. *J. Virol.* 86, 9416–9431.
- Villhauer, E.B., Brinkman, J.A., Naderi, G.B., Burkey, B.F., Dunning, B.E., Prasad, K., Mangold, B.L., Russell, M.E., Hughes, T.E., 2003. 1-[[[(3-Hydroxy-1-adamantyl)amino]acetyl]-2-cyano-(S)-pyrrolidine]: a potent, selective, and orally bioavailable dipeptidyl peptidase IV inhibitor with antihyperglycemic properties. *J. Med. Chem.* 46, 2774–2789.
- Wang, J., Ma, C., Fiorin, G., Carnevale, V., Wang, T., Hu, F., Lamb, R.A., Pinto, L.H., Hong, M., Klein, M.L., DeGrado, W.F., 2011a. Molecular dynamics simulation directed rational design of inhibitors targeting drug-resistant mutants of influenza A virus M2. *J. Am. Chem. Soc.* 133, 12834–12841.
- Wang, J., Qui, J.X., Soto, C., DeGrado, W.F., 2011b. Structural and dynamic mechanisms for the function and inhibition of the M2 proton channel from influenza A virus. *Curr. Opin. Struct. Biol.* 21, 68–80.
- Wang, J., Wu, Y., Ma, C., Fiorin, G., Wang, J., Pinto, L.H., Lamb, R.A., Klein, M.L., DeGrado, W.F., 2013. Structure and inhibition of the drug-resistant S31N mutant of the M2 ion channel of influenza A virus. *Proc. Natl. Acad. Sci. USA* 110, 1315–1320.
- Zhang, W., Xu, J., Liu, F., Li, C., Jie, Y., Chen, S., Li, Z., Liu, J., Chen, L., Zhou, G., 2010a. Heterodimers of histidine and amantadine as inhibitors for wild type and mutant M2 channels of influenza A. *Chin. J. Chem.* 28, 1417–1423.
- Zhang, W., Qi, J., Shi, Y., Li, Q., Gao, F., Sun, Y., Lu, X., Lu, Q., Vavricka, C.J., Liu, D., Yan, J., Gao, G.F., 2010b. Crystal structure of the swine-origin A (H1N1)-2009 influenza A virus hemagglutinin (HA) reveals similar antigenicity to that of the 1918 pandemic virus. *Protein Cell* 1, 459–467.